Journal of Enzyme Inhibition and Medicinal Chemistry, August 2008; 23(4): 445–453

Three-dimensional quantitative structure-activity relationship (CoMFA and CoMSIA) studies on galardin derivatives as gelatinase A (matrix metalloproteinase 2) inhibitors

JIANBIN ZHENG[1,2], REN WEN[1,2], & DOMINIQUE GUILLAUME[3,†]

[1]*School of Pharmacy, East China University of Science and Technology, Shanghai, 200237, P. R. China,* [2]*School of Pharmacy, Fudan University, Shanghai 200032, P. R. China, and* [3]*Faculté de Pharmacie, FRE 2715 CNRS, Université de Reims Champagne-Ardenne, Reims 51100, France*

(Received 9 May 2007; in final form 6 August 2007)

Abstract
Three-dimensional quantitative structure-activity relationship models have been derived using comparative molecular field analysis (CoMFA), comparative molecular similarity indices analysis (CoMSIA) and molecule docking for the training sets of galardin-based matrix metalloproteinase inhibitors (MMPIs). The statistical values for the best models are significant. The models showed that the steric effect near the S1′ pocket and hydrogen-bonding effect of the zinc binding group play key roles on the inhibitory activity of gelatinase A. The sets of the training and test proved the models were stable and predictive, and may have a good prediction for the inhibition activities of galardin derivatives as gelatinase A inhibitors. The results not only lead to a better understanding of the molecular mechanisms and structural requirements of gelatinase A inhibitors but also can help to design novel inhibitors against gelatinase A.

Keywords: *3D-QSAR, CoMFA, CoMSIA, gelatinase A, matrix metalloproteinase 2, Galardin, inhibition, MMP-2*

Introduction

Matrix Metalloproteinase (MMPs) comprise a family of over 20 zinc endopeptidases that can degrade virtually all the constituents of the extracellular matrix, including gelatin, fibronectin, laminin, basement membrane, interstitial collagens, and proteoglycan [1–4]. MMPs are active in a number of disease processes including tumor metastasis [5], periodontal disease [6], multiple sclerosis [7], congestive heart failure [8], and degenerative diseases such as osteo- and rheumatoid arthritis [9]. This association has created an intense search for potent MMP inhibitors as potential therapeutics. Inhibitors of gelatinase A (MMP2) are potentially valuable as inhibitors of tumor metastasis [10,11]. A large number of potent inhibitors have been discovered and some have been tested in clinical trials as therapies for cancer and arthritis with great expectations.

The broad-spectrum matrix metalloprotease inhibitor galardin (GM 6001, Ilomastat) is a hydroxamic acid originally synthesized as an inhibitor of human skin collagenase [12], and has been shown to widely inhibit MMP 1, 2, 3, and 9 [13]. Several strategies have been applied to the modification of galardin, for example, the non-hydroxamic acid derivatives present potent selectivity for MMP2 versus MMP1 [14].

A large number of MMP crystal structures, as well as several NMR studies have been reported since 1994 [15]. These structures revealed subtle differences in the active site of MMPs that have been

Correspondence: R. Wen, School of Pharmacy, Fudan University, Shanghai 200032, P. R. China. Tel: 86 21 54237560. Fax: 86 21 64033265. E-mail: rwen@shmu.edu.cn
†Tel/Fax: 33 326918473. E-mail: dominique.guillaume@univ-reims.fr

ISSN 1475-6366 print/ISSN 1475-6374 online
DOI: 10.1080/14756360701632221

Table I. Structures and MMP2 inhibitory activity of compounds used in test set.

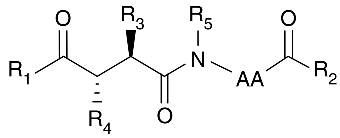

No.	R_1	R_2	R_3	R_4	R_5	AA*	Experimental (pIC_{50})
1	NHOH	$NHCH_3$	i-Bu	H	H	L-Trp	9.398
2	$NHOCH_3$	$NHCH_3$	i-Bu	H	H	L-Trp	8.201
3	NHOBu	$NHCH_3$	i-Bu	H	H	L-Trp	7.959
4	$NHOCH_2OCOCH_3$	$NHCH_3$	i-Bu	H	H	L-Trp	4.149
5	NHOH	$NHCH_3$	i-Bu	OH	H	L-Trp	9.051
6	NHOH	$NHCH_3$	i-Bu	H	H	L-*tert*-Leu	8.959
7	NHOH	$NHCH_3$	i-Bu	OH	H	L-*tert*-Leu	9.328
8	NHOH	$NHCH_3$	Bu	H	H	L-Trp	9.244
9	NHOH	$NHCH_3$	Hex	H	H	L-Trp	9.678
10	NHOH	$NHCH_3$	Oct	H	H	L-Trp	9.180
11	NHOH	$NHCH_3$	O-iPr	H	H	L-Trp	7.377
12	NHOH	$NHCH_3$	O-Pen	H	H	L-Trp	7.367
13	NHOH	$NHCH_3$	i-Bu	H	CH_3	L-Trp	7.770
14	NHOH	$NHCH_3$	i-Bu	H	H	L-3-Bal	9.357
15	NHOH	$NHCH_3$	i-Bu	H	H	L-1-Nal	9.377
16	NHOH	$NHCH_3$	i-Bu	H	H	L-2-Nal	9.155
17	NHOH	$NHCH_3$	i-Bu	H	H	L-3-Qal	9.000
18	NHOH	$NHCH_3$	i-Bu	H	H	L-8-Qal	8.886
19	NHOH	$NHCH_3$	i-Bu	H	H	L-4,4′-Bip	8.398
20	NHOH	$NHCH_3$	i-Bu	H	H	L-Phe	9.155
21	NHOH	$NHCH_3$	i-Bu	H	H	L-4-Pal	9.018
22	NHOH	$NHCH_3$	i-Bu	H	H	L-2-Ptp	10.036
23	NHOH	$NH(CH_2)_4CH_3$	i-Bu	H	H	L-Trp	8.337
24	NHOH	$NH(CH_2)_2OH$	i-Bu	H	H	L-Trp	9.357
25	NHOH	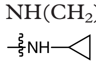	i-Bu	H	H	L-Trp	9.056
26	NHOH	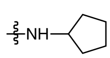	i-Bu	H	H	L-Trp	8.585
27	NHOH	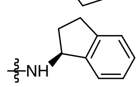	i-Bu	H	H	L-Trp	7.721
28	NHOH	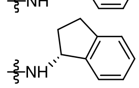	i-Bu	H	H	L-Trp	6.620
29	NHOH	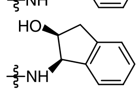	i-Bu	H	H	L-Trp	8.125
30	NHOH	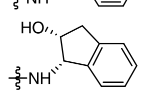	i-Bu	H	H	L-Trp	7.337
31	NHOH	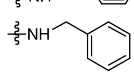	i-Bu	H	H	L-Trp	8.699
32	NHOH	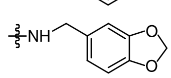	i-Bu	H	H	L-Trp	8.161
33	NHOH	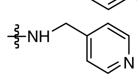	i-Bu	H	H	L-Trp	9.222
34	NHOH	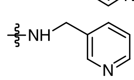	i-Bu	H	H	L-Trp	9.284
35	NHOH	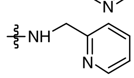	i-Bu	H	H	L-Trp	9.268
36	NHOH	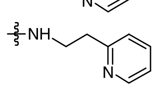	i-Bu	H	H	L-Trp	9.137
37	NHOH	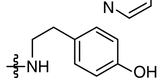	i-Bu	H	H	L-Trp	9.284
38	NHOH	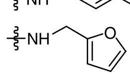	i-Bu	H	H	L-Trp	9.036

Table I – *continued*

No.	R_1	R_2	R_3	R_4	R_5	AA*	Experimental (pIC_{50})
39	NHOH	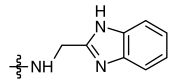	i-Bu	H	H	L-Trp	8.137
40	NHOH	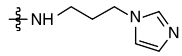	i-Bu	H	H	L-Trp	8.886
41	NHOH	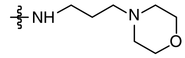	i-Bu	H	H	L-Trp	9.149
42	NHOH	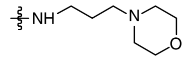	i-Bu	H	CH_3	L-Trp	7.260
43	NHOH	$N(CH_3)_2$	i-Bu	H	H	L-Trp	7.721
44	NHOH	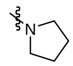	i-Bu	H	H	L-Trp	7.699
45	NHOH	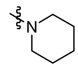	i-Bu	H	H	L-Trp	7.721
46	NHOH	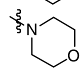	i-Bu	H	H	L-Trp	8.456
47	NHOH	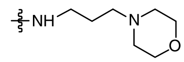	i-Bu	H	H	L-1-Nal	9.229
48	NHOH	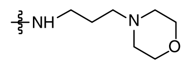	i-Bu	H	H	L-2-Nal	8.523
49	NHOH	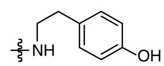	i-Bu	H	H	L-2-Nal	8.092
50	NHOH	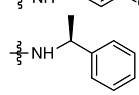	i-Bu	H	H	L-2-Nal	7.886
51	NHOH	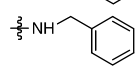	i-Bu	H	H	L-2-Nal	7.745
52	NHOH	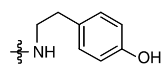	i-Bu	H	H	L-4,4′-Bip	8.092
53	NHOH	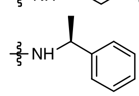	i-Bu	H	H	L-4,4′-Bip	7.602
54	NHOH	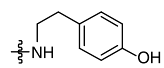	i-Bu	H	H	L-4-Pal	8.721
55	NHOH	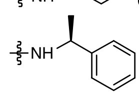	i-Bu	H	H	L-4-Pal	8.721
56	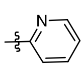	$NHCH_3$	i-Bu	H	H	L-Trp	6.745
57	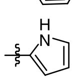	$NHCH_3$	i-Bu	H	H	L-Trp	6.268
58	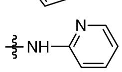	$NHCH_3$	i-Bu	H	H	L-Trp	7.301
59	$NHNH_2$	$NHCH_3$	i-Bu	H	H	L-Trp	6.260
60	$NHNH_2SO_2CH_3$	$NHCH_3$	i-Bu	H	H	L-Trp	6.131
61	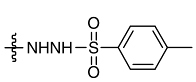	$NHCH_3$	i-Bu	H	H	L-Trp	7.620
62	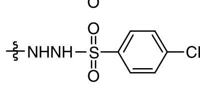	$NHCH_3$	i-Bu	H	H	L-Trp	7.745
63	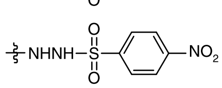	$NHCH_3$	i-Bu	H	H	L-Trp	6.509
64	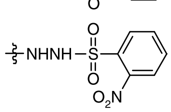	$NHCH_3$	i-Bu	H	H	L-Trp	6.495

Table I – *continued*

No.	R_1	R_2	R_3	R_4	R_5	AA*	Experimental (pIC_{50})
65	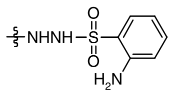	$NHCH_3$	i-Bu	H	H	L-Trp	7.036
66	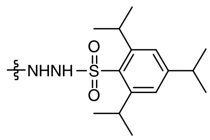	$NHCH_3$	i-Bu	H	H	L-Trp	7.000
67	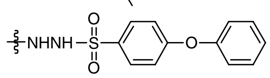	$NHCH_3$	i-Bu	H	H	L-Trp	7.347
68	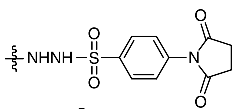	$NHCH_3$	i-Bu	H	H	L-Trp	7.102
69	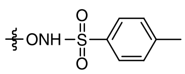	$NHCH_3$	i-Bu	H	H	L-Trp	5.699
70	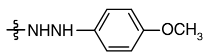	$NHCH_3$	i-Bu	H	H	L-Trp	5.000
71	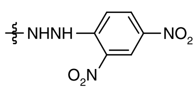	$NHCH_3$	i-Bu	H	H	L-Trp	5.000
72	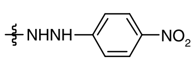	$NHCH_3$	i-Bu	H	H	L-Trp	5.000
73†	OH	$NHCH_3$	i-Bu	H	H	L-Trp	7.004
74†	NHOH	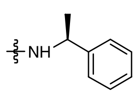	i-Bu	H	H	L-Trp	9.194
75†	NHOH	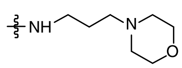	i-Bu	H	H	L-4,4′-Bip	8.174
76†	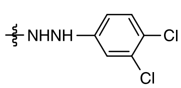	$NHCH_3$	i-Bu	H	H	L-Trp	5.000
77†	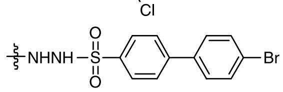	$NHCH_3$	i-Bu	H	H	L-Trp	7.009

* See Table II; † Compounds those were not included in the construction of the 3D-QSAR models.

exploited for the design of specific inhibitors. But the works on MMP2 were relatively limited, only one NMR resolution has been determined till now [16]. Comparative molecular field analysis (CoMFA) [17] and comparative molecular similarity indices analysis (CoMSIA) [18], regarded as industry standards for constructing three-dimensional quantitative structure-activity relationship (3D-QSAR) models, have been established in many studies as powerful tools in rational drug design and related applications [19].

In this work, we carried out a 3D-QSAR (CoMFA and CoMSIA) study on galardin derivatives in order to establish the molecular structure-MMP2 inhibition relationship. The obtained models will give some insight into how steric, electrostatic, hydrophobic and hydrogen bonding interactions influence MMP2 inhibition. These could lead to a better understanding of the molecular mechanisms and structural requirements of MMP2 inhibitors, and thus used to design more potent inhibitors.

Materials and methods

Dataset for analysis

Biological data were taken from the literatures [14,20] and one of the laboratory (some data were not published), and were randomly separated into two subsets; 72 and 5 compounds for training and test sets, respectively. Although the biological activities of compounds were taken from different sources, both of the laboratories selected galardin as positive control with same activity. Likewise to the previous QSAR studies, all compounds were combined together based on the assumption that methods and conditions of activity testing were similar. The structures of the training and test set molecules are given in Tables I and II.

Table II. Structures of AA.

Abbreviation	AA
L-Trp	L-tryptophan
L-3-Bal	L-3-(3-benzothienyl)-alanine
L-1-Nal	L-3-(1-naphthyl)-alanine
L-2-Nal	L-3-(2-naphthyl)-alanine
L-3-Qal	L-3-(3-quinolyl)-alanine
L-8-Qal	L-3-(8-quinolyl)-alanine
L-4,4′-Bip	L-3-(4,4′-biphenyl)-alanine
L-Phe	L-3-phenylalanine
L-3-Pal	L-3-(3-pyridyl)-alanine
L-4-Pal	L-3-(4-pyridyl)-alanine
L-*tert*-Leu	L-*tert*-leucine
L-Abr	L-abrine
L-2-Ptp	L-2-phenyltryptophan

The biological activities were converted into the corresponding pIC_{50} values.

$$pIC_{50} = -\log IC_{50}$$

Alignment method

All the molecular modeling studies, CoMFA and CoMSIA reported herein were performed using SYBYL 6.8 [21]. The initial conformation of the galardin was derived by some modifications from the inhibitor of 1HV5 (MMP11) in RCSB Protein Data Bank (PDB) because of their similar structures and binding manner. The bioactive conformation of galardin had been proposed [20], which is proved to be similar to the inhibitor in 1HV5. Then, the conformation of the galardin was used as a template molecule for the construction of the remaining data series. The final conformations of the galardin and its derivatives were achieved by docking them into the crystal structure of MMP2 (1HOV) with DOCK 5.0 [22]. The compounds were aligned to galardin basing on their similar framework.

CoMFA calculations

The grid spacing was set to 2.0 Å. Both the steric and the electrostatic fields were calculated for each molecule using a carbon sp^3 probe atom with a charge of +1, and energy cutoff was set to 30 kcal/mol. The partial atomic charges for each compound were assigned by the GasteigereMarsili method.

CoMSIA calculations

CoMSIA analyses were conducted focusing on hydrogen-bond donor/acceptor fields, with similarity indices computed using a sp3 carbon with a + 1 charge, +1 radius, and +1 hydrophobicity. The attenuation factor R was set to 0.3 for the Gaussian-type distance dependence.

Partial least square analysis

PLS is used to correlate the MMP2 inhibitory activity with the CoMFA and CoMSIA values containing the magnitude of steric, electrostatic, and other potentials. Crossvalidation yielded the optimum number of principal components, together with the highest cross-validated r^2_{cv} value. The PLS analyses were then repeated without cross-validation using the optimum number of principal components, giving final CoMFA and CoMSIA models from which the conventional r^2 values, non-cross-validated standard error estimate (*SSE*), *F* ratios and related statistical parameters were computed. A column filtering of 2.0 kcal/mol was applied to reduce the noise and to speed up the calculation. CoMFA standard scaling was applied to all of the CoMFA analysis, and autoscaling was applied to all CoMSIA analyses.

Testing of 3D-QSAR Models

To test the stability and predictive ability of the 3D-QSAR results, five analogous compounds 73–77 which were not included in the construction of CoMFA and CoMSIA models, were selected as a set of testing for validation. These molecules were aligned to the template and their activities were predicted.

Results and discussion

CoMFA statistics

Aligning the complete data set of 72 compounds to galardin yielded internally predictive CoMFA models in terms of cross-validated r^2_{cv} (0.524) and conventional r^2 (0.830). However, the standard error of estimate *SEE* for this simulation was high (0.533). Ligand 4 with a longer chain substituted zinc binding group (ZBG) demonstrate virtually no activity against MMP2 ($IC_{50} \sim 71\,000$ nM). Ligands 11 and 12 with alkyloxy P1′ groups showed less activity against MMP2 when comparing to ligands 1, 9 and 10 with alkyl P1′ groups. It was also observed from the docking study (data not given) that these alkyloxy P1′ groups were not fitted well into the S1′ binding site. Excluding ligands 4, 11 and 12 from the model, the best CoMFA model was obtained with a cross-validation r^2_{cv} value of 0.712. The conventional correlation coefficient r^2 value was 0.970, $F = 255.927$, n = 4 and standard error estimate (*SSE*) was 0.216.

CoMFA contours

The best CoMFA model was used to generate the 3D contour maps to represent the QSAR result. The follow figures show a stereocolors views of 3D steric and electrostatic map.

The big green polyhedron near iso-butyl group (Figure 1) inserted into S1′ pocket, show

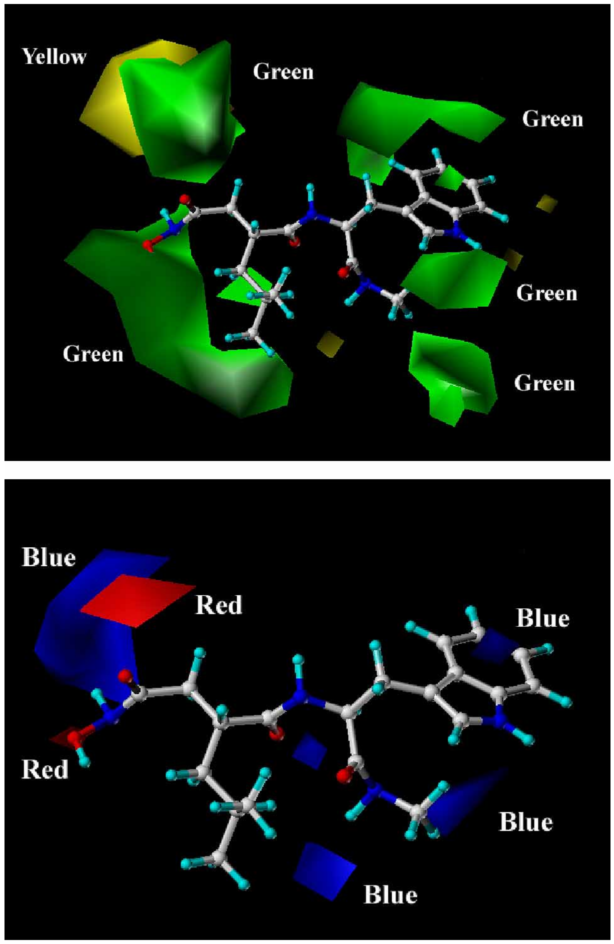

Figure 1. CoMFA contour maps for the partial training set (ligands 4, 11 and 12 omitted) of galardin derivatives, and shown with compound 1. Colored polyhedra represent areas on or near the ligand where properties correlate strongly with an increase in binding affinity. Red: negative electrostatic potential; blue: positive electrostatic potential; yellow: negative steric potential; green: positive steric potential.

more steric group is favorable, which may due to the deep S1′ pocket in MMP2. Compound 22 possessing a phenyl group at the 2 position of the indole ring exhibited more active than galardin as the green polyhedron occurred in the close area, which may contribute to the formation of lipophilic contact between phenyl substitute and the isoleucine nearby. Adding bulky substituents to the R2 group and transforming the tryptophan to other amino acids are tolerable because the S2′ and S3′area are open and solvent-exposed as the green polyhedron near to these groups indicated. The yellow polyhedron adjacent to R1 group does not affect the activity obviously. From the results of the CoMFA model, the steric effect is proved the great influence on the inhibitory activities against MMP2.

The electrostatic contours of CoMFA (Figure 1) shows red contour enclosing the two oxygens of hydroxamate zinc binding group (ZBG) where high electron density is expected to increase the activity. As expected, the hydroxamate galardin derivatives possess a clear potency advantage than non-hydroxamate derivatives, as shown in the Table I. The electrostatic contours also give blue polyhedra in the vicinity of protonated nitrogen where low electron density is expected to increase activity. Ligands 56, 57 exhibit low activities because they don't possess the nitrogen with the ZBG.

CoMSIA statistics

Similar to CoMFA model, the alignment of the complete training set of 72 compounds to galardin yielded internally predictive CoSIA models in terms of cross-validated r^2_{cv} (0.480) and conventional r^2 (0.674). However, the standard error of estimate *SEE* for this simulation was very high (0.744). Excluding ligands 4, 11 and 12 from the model, the best CoMSIA model was obtained with a cross-validation r^2_{cv} value of 0.626. The conventional correlation coefficient r^2 value was 0.950, $F = 196.630$, the standard error of estimate (*SEE*) for this simulation was 0.280, which were significant for the CoMSIA models. When comparing with the best CoMFA model, these data showed some fewer significations, which may due to the diversity of R1 groups. While, the CoMFA model didn't give as much information as CoMSIA model did on this area.

CoMSIA contours

The CoMSIA contour map offers valuable information as to the hydrogen-bonding environment of the MMP2 active site (Figure 2), especially the zinc-chelating region. The hydrogen bond acceptor

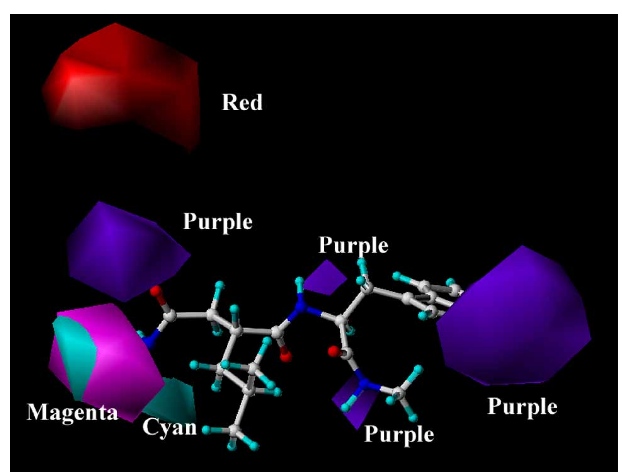

Figure 2. CoMSIA contour map for the partial training set (ligands 4, 11 and 12 omitted) of galardin derivatives, and shown with compound 1. Colored polyhedra represent areas on or near the ligand where hydrogen bonding correlates strongly with binding affinity. Cyan: hydrogen-bond donors favored; purple: hydrogenbond donors disfavored; magenta: hydrogen-bond acceptors favored; red: hydrogen-bond acceptors disfavored.

Table III. Predicted Activities vs Experimental Activities (pIC_{50}) and Residues by the model of CoMFA and CoMSIA.

		Predicted pIC_{50}		Residues	
No.	Experimental pIC_{50}	CoMFA	CoMSIA	CoMFA	CoMSIA
1	9.398	8.932	9.620	0.466	−0.222
2	8.201	8.285	7.958	−0.084	0.243
3	7.959	8.002	8.136	−0.043	−0.177
5	9.051	9.062	9.534	−0.011	−0.483
6	8.959	9.216	8.854	−0.257	0.105
7	9.328	8.998	9.270	0.33	0.058
8	9.244	9.233	9.279	0.011	−0.035
9	9.678	9.784	9.972	−0.106	−0.294
10	9.180	9.453	9.243	−0.273	−0.063
13	7.770	8.055	7.584	−0.285	0.186
14	9.357	9.095	9.749	0.262	−0.392
15	9.377	9.145	9.014	0.232	0.363
16	9.155	8.893	9.177	0.262	−0.022
17	9.000	8.861	8.625	0.139	0.375
18	8.886	9.028	8.981	−0.142	−0.095
19	8.398	8.507	8.349	−0.109	0.049
20	9.155	9.042	8.761	0.113	0.394
21	9.018	9.344	9.192	−0.326	−0.174
22	10.036	9.817	9.516	0.219	0.52
23	8.337	8.533	7.791	−0.196	0.546
24	9.357	9.171	9.138	0.186	0.219
25	9.056	9.253	9.003	−0.197	0.053
26	8.585	8.486	8.525	0.099	0.06
27	7.721	7.307	7.643	0.414	0.078
28	6.620	6.588	6.879	0.032	−0.259
29	8.125	8.134	8.298	−0.009	−0.173
30	7.337	7.162	6.936	0.175	0.401
31	8.699	8.647	8.533	0.052	0.166
32	8.161	7.885	7.971	0.276	0.19
33	9.222	9.328	9.159	−0.106	0.063
34	9.284	9.075	8.990	0.209	0.294
35	9.268	9.344	9.265	−0.076	0.003
36	9.137	9.305	9.189	−0.168	−0.052
37	9.284	9.279	9.200	0.005	0.084
38	9.036	9.254	9.090	−0.218	−0.054
39	8.137	8.176	8.255	−0.039	−0.118
40	8.886	8.794	8.976	0.092	−0.09
41	9.149	8.938	8.883	0.211	0.266
42	7.260	7.209	7.259	0.051	0.001
43	7.721	7.986	8.204	−0.265	−0.483
44	7.699	7.627	8.092	0.072	−0.393
45	7.721	8.201	8.540	−0.48	−0.819
46	8.456	8.245	8.140	0.211	0.316
47	9.229	9.255	9.052	−0.026	0.177
48	8.523	8.683	8.630	−0.16	−0.107
49	8.092	8.225	7.792	−0.133	0.3
50	7.886	7.931	8.126	−0.045	−0.24
51	7.745	7.558	7.474	0.187	0.271
52	8.092	8.031	8.188	0.061	−0.096
53	7.602	7.869	8.026	−0.267	−0.424
54	8.721	8.825	8.840	−0.104	−0.119
55	8.721	8.557	8.762	0.164	−0.041
56	6.745	6.707	6.981	0.038	−0.236
57	6.268	6.672	6.250	−0.404	0.018
58	7.301	6.895	6.999	0.406	0.302
59	6.260	6.496	6.497	−0.236	−0.237
60	6.131	6.356	5.808	−0.225	0.323
61	7.620	7.563	7.316	0.057	0.304
62	7.745	7.642	7.862	0.103	−0.117
63	6.509	6.462	6.456	0.047	0.053
64	6.495	6.286	6.624	0.209	−0.129
65	7.036	6.958	6.753	0.078	0.283
66	7.000	7.373	6.767	−0.373	0.233

Table III – *continued*

No.	Experimental pIC_{50}	Predicted pIC_{50}		Residues	
		CoMFA	CoMSIA	CoMFA	CoMSIA
67	7.347	7.269	7.391	0.078	−0.044
68	7.102	7.093	7.236	0.009	−0.134
69	5.699	6.062	5.939	−0.363	−0.24
70	5.000	4.995	5.553	0.005	−0.553
71	5.000	5.015	5.101	−0.015	−0.101
72	5.000	4.817	5.078	0.183	−0.078
73*	7.004	7.276	7.523	−0.272	−0.519
74*	9.194	9.038	8.887	0.156	0.307
75*	8.174	8.658	8.712	−0.484	−0.538
76*	5.000	5.497	5.763	−0.497	−0.763
77*	7.009	6.626	7.231	0.383	−0.222

* Compounds those were not included in the construction of the 3D-QSAR models.

contours (Figure 2) show presence of big magneta contours close to the ZBG of the template molecule, where a hydrogen-bond acceptor at this location to engage in zinc binding is necessary. One large cyan contour protonated hydroxamate nitrogen and hydrazide nitrogen indicates favorable hydrogen-bond donation from these compounds to the Glu121 charged side chain. Whereas, the hydrogenbond in the rest part of galardin derivatives only manifests unfavorable effect. The red polyhedron suggests that the hydrogen bond acceptor at the phenyl of R1 group is disfavored. Ligands 63, 71, 72 exhibited less active comparing to the ligands 61 and 62. And the purple polyhedron near some part of the galardin indicates hydrogen bond donors disfavored.

Predictability and validation of the models

The actual, predicted and residual values of training and test set for CoMFA and CoMSIA are given in Table III, and the predicted pIC_{50} values are in good agreement with the experimental data in a statistically tolerable error range. The plots of calculated vs. observed activity values for training set molecules and predicted vs. observed activity values for the test set molecules are shown in Figure 3. It was clear that the predicted activity values showed close correlation to the observed ones.

According to these results, the developed CoMFA and CoMSIA models exhibited strong predictability on galardin derivatives, and were therefore enough to guide the design of new molecules.

Conclusions

We have developed the 3D-QSAR models of the galardin derivatives as MMP2 inhibitors by CoMFA and CoMSIA methods. The conformations of the galardin derivatives were derived from the inhibitor conformation in MMP11 (1HV5, PDB).

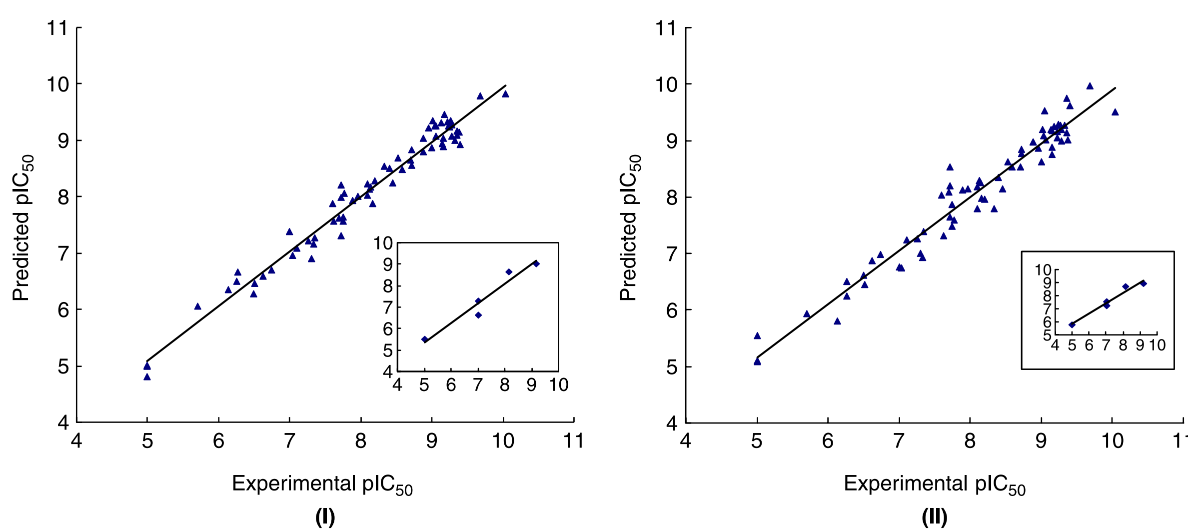

Figure 3. Correlation between predicted activities (pIC_{50}) and the experimental activities (pIC_{50}) from CoMFA (I) and CoMSIA (II) analyses. ▲, compounds of the training set; ■, compounds of the test set.

The 3D-QSAR studies combining with molecule docking were successfully applied in this research by some modifications. The best CoMFA model was obtained with a cross-validation r_{cv}^2 value of 0.712, the conventional correlation coefficient r^2 value was 0.970, and the best CoMSIA model was obtained with a cross-validation r_{cv}^2 value of 0.626, the conventional correlation coefficient r^2 value was 0.950. The steric effect near S1′ pocket derived from CoMFA model and the hydrogen-bonding effect of ZBG from CoMSIA model revealed the great importance for the MMP2 inhibitory activity. The contour maps produced by CoMFA and CoMSIA may help to understand the structure requirements for the inhibitors against MMP2, and design the novel MMP2 inhibitors.

Acknowledgements

The main part of this work was finished in Université de Reims. Jianbin Zheng is grateful for the French government scholarship provided by the Consulat Général de France à Shanghai.

References

[1] Malemud CJ. Matrix metalloproteinases (MMPs) in health and disease: An overview. Front Biosci 2006;11:1696–1701.
[2] Wang JC. Importance of plasma matrix metalloproteinases (MMP) and tissue inhibitors of metalloproteinase (TIMP) in development of fibrosis in agnogenic myeloid metaplasia. Leuk Lymphoma 2005;46:1261–1268.
[3] Hartenstein B, Dittrich BT, Stickens D, Heyer B, Vu TH, Teurich S, Schorpp-Kistner M, Werb Z, Angel P. Epidermal development and wound healing in matrix metalloproteinase 13-deficient mice. J Invest Dermatol 2006;126:486–496.
[4] Whittaker M, Floyd CD, Brown P, Gearing AJH. Design and therapeutic application of matrix metalloproteinase inhibitors. Chem Rev 1999;99:2735–2776.
[5] Chetty C, Bhoopathi P, Joseph P, Chittivelu S, Rao JS, Lakka S. Adenovirus-mediated small interfering RNA against matrix metalloproteinase-2 suppresses tumor growth and lung metastasis in mice. Mol Cancer Ther 2006;5:2289–2299.
[6] Ilgenli T, Vardar-Sengul S, Gurkan A, Sorsa T, Stackelberg S, Kose T, Atilla G. Gingival crevicular fluid matrix metalloproteinase-13 levels and molecular forms in various types of periodontal diseases. Oral Dis 2006;12:573–579.
[7] van Horssen J, Vos CMP, Admiraal L, van Haastert ES, Montagne L, van der Valk P, de Vries HE. Matrix metalloproteinase-19 is highly expressed in active multiple sclerosis lesions. Neuropathol Appl Neurobiol 2006;32: 585–593.
[8] Thorud HMS, Stranda A, Birkeland JA, Lunde PK, Sjaastad I, Kolset SO, Sejersted OM, Iversen PO. Enhanced matrix metalloproteinase activity in skeletal muscles of rats with congestive heart failure. Am J Physiol Regul Integr Comp Physiol 2005;289:R389–R394.
[9] Liu MZ, Sun HJ, Wang XF, Koike T, Mishima H, Ikeda K, Watanabe T, Ochiai N, Fan HL. Association of increased expression of macrophage elastase (Matrix metalloproteinase 12) with rheumatoid arthritis. Arthritis Rheum 2004;50: 3112–3117.
[10] Qu XJ, Yuan YX, Xu WF, Chen MH, Cui SX, Meng H, Li Y, Makuuchi M, Nakata M, Tang W. Caffeoyl pyrrolidine derivative LY52 inhibits tumor invasion and metastasis via suppression of matrix metalloproteinase activity. Anticancer Res 2006;26:3573–3578.
[11] Qu XJ, Yuan YX, Tian ZG, Xu WF, Chen MH, Cui SX, Guo Q, Gai RY, Makuuchi M, Nakata M, Tang W. Using caffeoyl pyrrolidine derivative LY52, a potential inhibitor of matrix metalloproteinase-2, to suppress tumor invasion and metastasis. Int J Mol Med 2006;18:609–614.
[12] Grobelny D, Poncz L, Galardy RE. Inhibition of human skin fibroblast collagenase, thermolysin, and pseudomonas-aeruginosa elastase by peptide hydroxamic acids. Biochemistry 1992;31:7152–7154.
[13] Agren MS, Mirastschijski U, Karlsmark T, Saarialho-Kere UK. Topical synthetic inhibitor of matrix metalloproteinases delays epidermal regeneration of human wounds. Exp Dermatol 2001;10:337–348.
[14] Auge F, Hornebeck W, Decarme M, Laronze JY. Improved gelatinase A selectivity by novel zinc binding groups containing galardin derivatives. Bioorg Med Chem Lett 2003;13: 1783–1786.
[15] Rao BG. Recent developments in the design of specific matrix metalloproteinase inhibitors aided by structural and computational studies. Curr Pharm Des 2005;11:295–322.
[16] Feng YQ, Likos JJ, Zhu LM, Woodward H, Munie G, McDonald JJ, Stevens AM, Howard CP, De Crescenzo GA, Welsch D, Shieh HS, Stallings WC. Solution structure and backbone dynamics of the catalytic domain of matrix metalloproteinase-2 complexed with a hydroxamic acid inhibitor. BBA-Proteins Proteomics 2002;1598:10–23.
[17] Cramer R, Patterson D, Bunce J. Effect of shape on binding of steroids to carrier proteins. J Am Chem Soc 1988;110: 5959–5967.
[18] Klebe G, Abraham U, Mietzner T. Molecular similarity indices in a comparative analysis (CoMSIA) of drug molecules to correlate and predict their biological activity. J Med Chem 1994;37:4130–4146.
[19] Puntambekar DS, Giridhar R, Yadav MR. Understanding the antitumor activity of novel tricyclicpiperazinyl derivatives as farnesyltransferase inhibitors using CoMFA and CoMSIA. Eur J Med Chem 2006;41:1279–1292.
[20] Levy DE, Lapierre F, Liang WS, Ye WQ, Lange CW, Li XY, Grobelny D, Casabonne M, Tyrrell D, Holme K, Nadzan A, Galardy RE. Matrix metalloproteinase inhibitors: A structure-activity study. J Med Chem 1998;41:199–223.
[21] Tripos, Inc., St. Louis, MO.
[22] Kuntz ID, Blaney JM, Oatley SJ, Langridge R, Ferrin TE. A geometric approach to macromolecule-ligand interactions. J Mol Biol 1982;161:269–288.